Spectroscopic ellipsometry studies of HF treated Si (100) surfaces

Huade Yao and John A. Woollam
University of Nebraska, Center for Microelectronic and Optical Materials Research, and Department of Electrical Engineering, Lincoln, Nebraska 68588-0511

Samuel A. Alterovitz
NASA Lewis Research Center, Cleveland, Ohio 44135

(Received 26 October 1992; accepted for publication 3 April 1993)

Both *ex situ* and *in situ* spectroscopic ellipsometry (SE) measurements have been employed to investigate the effects of HF cleaning on Si surfaces. The hydrogen-terminated (H-terminated) Si surface was modeled as an equivalent dielectric layer, and monitored in real time by SE measurements. The SE analyses indicate that after a 20-s 9:1 HF dip without rinse, the Si (100) surface was passivated by the hydrogen termination and remained chemically stable. Roughness of the HF-etched bare Si (100) surface was observed, in an ultrahigh vacuum (UHV) chamber, and analyzed by the *in situ* SE. Evidence for desorption of the H-terminated Si surface-layer, after being heated to ~550 °C in the UHV chamber, is presented and discussed. This is the first use of an *ex situ* and *in situ* real-time, nondestructive technique capable of showing state of passivation, the rate of reoxidation, and the surface roughness of the H-terminated Si surfaces.

In the fabrication of ultralarge-scale integrated circuits, preparation of native oxide free Si surfaces, the monitor and control of Si surface passivation and reoxidation are extremely important issues. Aqueous HF etching of Si surfaces removes the surface oxide and terminates the Si surface with atomic hydrogen.[1,2] The hydrogen termination retards the Si surface oxidation, and protects the surface from chemical attack.[3,4] Therefore, the HF cleaning of Si surfaces has received increasing attention. However, the properties of hydrogen-terminated (H-terminated) Si surfaces under various conditions, and the degree of surface passivation and reoxidation are still under investigation.[4–7] In this letter, we report results of *ex situ* and *in situ* spectroscopic ellipsometry (SE) studies of HF cleaned Si (100) surfaces.

SE is a surface-sensitive, nondestructive optical technique used to characterize surface overlayer thicknesses, multilayer structures, optical constants of bulk materials, and surface changes.[8,9] Ellipsometry determines the complex ratio of reflectance R_p to R_s, defined as

$$\rho = R_p/R_s = \tan(\psi)e^{i\Delta}, \tag{1}$$

where R_p and R_s are the reflection coefficient of light polarized parallel to (p) or perpendicular to (s) the plane of incidence, and the values of $\tan(\psi)$ and Δ are the amplitude and phase of the complex ratio.

The pseudodielectric function $\langle\epsilon\rangle$ can be obtained from the ellipsometrically measured values of ρ, assuming a two-phase model (ambient/substrate)[8] regardless of the possible presence of surface overlayers. For samples with surface overlayers or multilayer structures, SE data must be numerically fitted according to an assumed model (e.g., a three-phase model: ambient/surface overlayer/substrate). Assuming such a model, values of $\psi^c(h\nu_i,\Phi_j)$ and $\Delta^c(h\nu_i,\Phi_j)$, defined as in Eq. (1), are calculated. Here $h\nu$ is the photon energy and Φ is the external angle of incidence. A regression analysis is established to vary the model parameters (e.g., layers thicknesses) until the calculated and experimental values match as closely as possible. This process is done by minimizing the mean square error (MSE) function as described in Refs. 10 and 11. In our study, *ex situ* and *in situ* SE measurements were made using a Woollam Co. Variable Angle Spectroscopic Ellipsometer (VASE™), which was equipped with a beam-chopped, rotating analyzer to increase the stray light rejection and signal to noise ratio.

Si (100) surfaces covered with native oxide from a virgin p-type wafer of 14–22 Ω cm resistivity were employed to study the effects of HF treatments on Si. A piece from the wafer was dipped in 9:1 (volume ratio of deionized water to 49% HF) HF solution for approximately 20 s with no rinse. SE measurements were made in air, at a 75° angle of incidence, before and after the HF dip. During the measurement, the automated polarizer azimuth angle P was set to vary with changes of the measured $\psi(h\nu_i,\Phi_j)$ to minimize experimental errors in the ellip-

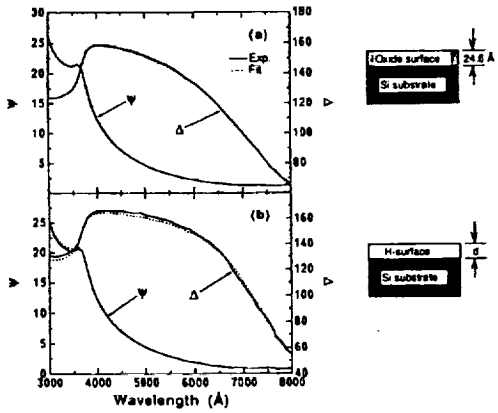

FIG. 1. Ψ and Δ values of *ex situ* SE measurements on a Si (100) surface: (a) before and (b) after the HF treatment. The solid line represents the experimental data, and the dashed line is the best fit of the SE analysis. Assumed models for the SE analysis, in each case, are sketched with the plots

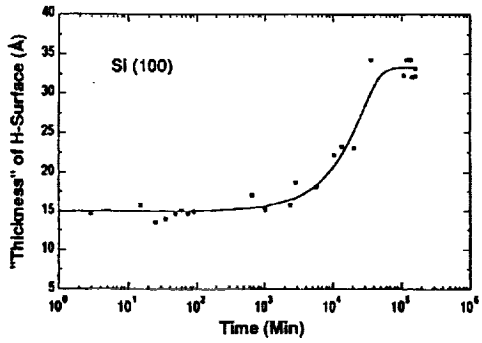

FIG. 2. Changes in effective thickness of the H-terminated Si surface (H surface) as a function of time, after the 20-s 9:1 HF dip, monitored by the *ex situ* SE measurements.

someter system.[12] It was set such that $P=\psi$ with $P_{\min}=10°$. The spectral scan, ranging from 3000 to 8000 Å, with an increment of 100 Å, was completed within 2–3 min. The SE analysis indicated that an approximately 25 Å thick native oxide covered the virgin Si surface as shown in Fig. 1(a). After the HF cleaning, the Si native oxides were removed and the Si surface was terminated with H-silicon bonds.[1,2] This H-terminated Si surface was modeled as an equivalent dielectric layer described by the optical constants of SiO_2[13] [for the SE analysis shown in Fig. 1(b)]. The optical constants of Si used for the calculations in the SE regression analysis are from Ref. 14. A typical "thickness" of the H-terminated Si surface (H surface) immediately after the HF cleaning, as indicated by the SE regression analysis, was in the range 14–17 Å. Notice that the thickness referred to here as an H surface was not the actual thickness of the H-surface layer, but the effective thickness of the modeled equivalent dielectric layer of SiO_2, which includes possible Si surface microroughness after HF etching (as discussed below). The value of this thickness as measured by SE was used to monitor the changes in the H surface.

SE measurements were made on this H surface in air at room temperature (RT) over a period of several months after the HF cleaning. Changes in thickness of the H surface were monitored as a function of time as shown in Fig. 2. The figure shows that the H-terminated Si surface remained unchanged for over 2 h, and very little reoxidation took place within 3–4 days. After two months the reoxidized Si surface layer saturates at a thickness of ~33 Å, which is thicker than the native oxide before the HF etching. The SE study indicates that remarkable surface passivation has been achieved by the hydrogen termination of Si surface dangling bonds, which contributes to the retardation of the Si surface oxidation during air exposure. The apparent larger thickness of the reoxidized layer provides a clue to the Si surface roughness after the HF etching.

In situ SE was employed to study changes of the H-terminated Si surface at elevated temperatures and the bare Si surface conditions after HF etching. During the *in situ* measurements, the ellipsometer was attached to an UHV chamber, fitted with a pair of low-strain fused-quartz

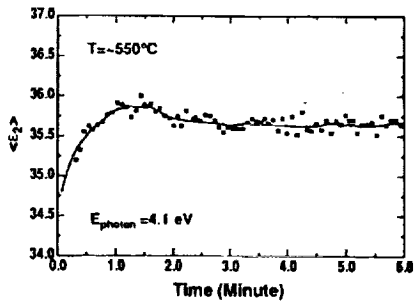

FIG. 3. Real time $\langle\epsilon_2\rangle$ data from the HF-treated Si (100) surface, inside the UHV chamber, at ~550 °C, near the E_2 critical-point energy.

windows.[11,15] A Si (100) sample was introduced into the UHV chamber, immediately after a 20-s 9:1 HF dip, and clamped on a resistor-heater plate that could be rotated and tilted by a rotary drive, inside the chamber. Temperatures were measured and controlled by two *K*-type thermocouples, which were calibrated by an infrared (IR) optical pyrometer. The typical base pressure of the UHV was $\sim 1\times 10^{-9}$ Torr.

The HF-cleaned Si (100) surface was heated to ~550 °C inside the UHV chamber, and real time ellipsometric measurements of one set of Ψ and Δ data were made periodically in time (about once every 5 s) at a photon energy of ~4.1 eV, corresponding to the critical point energy E_2 (i.e., ~4.1 eV for Si at ~550 °C),[16] while maintaining the sample at ~550 °C. These data were converted simultaneously to a pseudodielectric function $\langle\epsilon\rangle=\langle\epsilon_1\rangle+i\langle\epsilon_2\rangle$. In general, it has been established[9,11,15] that the peak value of the imaginary part $\langle\epsilon_2\rangle$ in semiconductors is very sensitive to the presence of surface overlayers (e.g., H surface) and any possible surface defects such as surface microscopic roughness. A reduction of the thickness of surface overlayer or surface roughness leads to increasing values of $\langle\epsilon_2\rangle$. The highest value $\langle\epsilon_2\rangle$ corresponds to the cleanest and smoothest bulk surface condition. Therefore, changes in the H surface induced at elevated temperatures can be monitored in real time by measuring the changes of $\langle\epsilon_2\rangle$.

Figure 3 shows changes in $\langle\epsilon_2\rangle$ in real time at

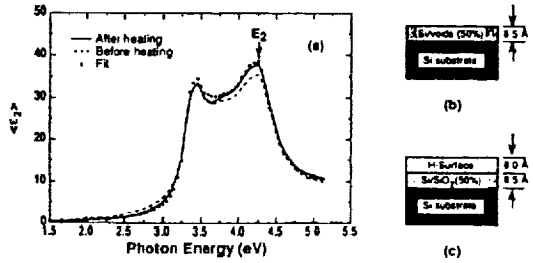

FIG. 4. (a) $\langle\epsilon_2\rangle$ spectrum of HF-treated Si at RT, measured by *in situ* SE, before (dashed line) and after (solid line) being heated to ~550 °C in the UHV chamber. The dotted line is the fit for the rough Si surface model, sketched in (b). (c) A sketch of the H-surface structure, containing the surface roughness formed by HF etching.

~ 550 °C. An obvious increase of $\langle \epsilon_2 \rangle$ within the first minute at ~ 550 °C indicates the desorption of H-terminated Si surface at ~ 550 °C. A flat plateau followed the desorption of the H surface indicates a stabilized Si surface. The plateau remained unchanged during further extended heating. This also suggests that there is no evidence of the surface quality deterioration (e.g., increasing surface roughness induced by heating) at this elevated temperature.[15]

SE data for the H-terminated Si surfaces were taken at RT before and after the heating, as shown in Fig. 4(a). A comparison of the two $\langle \epsilon_2 \rangle$ spectra at RT, shows a $\sim 7\%$ higher $\langle \epsilon_2 \rangle$ peak value at the E_2 critical point energy (~ 4.3 eV at RT) after the heating. This further confirms the desorption of the H surface after heating to ~ 550 °C. The evidence for desorption observed in this experiment is consistent with results obtained by thermally stimulated desorption measurements as described in Ref. 5.

The RT $\langle \epsilon_2 \rangle$ peak value at the E_2 energy after the desorption of the H surface, as shown in Fig. 4(a) (solid line), is considerably lower than the known value (~ 46) of Si from literature.[14] This indicates a roughened Si surface induced by the HF etching. The surface roughness was modeled as a top Si layer containing 50% voids, as shown in Fig. 4(b). The thickness of this rough Si layer was calculated by the regression analysis, under the assumption of the Bruggeman effective-medium approximation (EMA).[17] Good fit was obtained with a thickness of 8.5 Å, as shown in Fig. 4(a) (dotted line). It indicates an approximate 1–2 monolayer surface microroughness formed from the HF etching.

This model of rough Si surface was applied to characterize the H surface measured at RT in vacuum, before the heating, as shown in Fig. 4(c). In this case, the voids were replaced by SiO_2 to model the H termination of the rough Si layer, while the thickness of this rough layer was kept the same as in Fig. 4(b). On top of the rough Si surface, a pure H-surface layer was modeled and described by the optical constants of SiO_2, as we have discussed previously. The thickness of ~ 8 Å of this pure H-surface layer was calculated through the regression analysis. Notice that by modeling a rough interface between the top H surface and Si substrate, the top pure H surface has an effective thickness of ~ 8 Å, which is consistent with an expected monolayer H termination of Si surface.

Same surface-roughness model [as in Fig. 4(c)] was used to reanalyze the *ex situ* RT SE measurements shown in Fig. 1. The results show a reduced effective thickness of the initial top H surface, after the HF dip, of ~ 5.4 Å, and a saturated reoxide layer is ~ 21.7 Å. This value is quite consistent with the thickness of a fresh native oxide surface layer. The small difference between the two initial thicknesses of H surface (i.e., 8.0 and 5.4 Å) are likely due to different degrees of surface roughness of the two individual HF treated Si samples.

In summary, HF treated Si (100) surfaces were investigated by *ex situ* and *in situ* SE measurements. The SE analysis indicated that the Si (100) surface was well passivated via a ~ 20-s 9:1 HF dip with no rinse. Real-time SE data showed evidence for desorption of the H-terminated Si surfaces at ~ 550 °C in the UHV chamber. Si (100) surface roughness induced by HF etching was observed in a UHV chamber, and analyzed by the *in situ* SE. It was shown that a ~ 1–2 monolayer surface roughness was formed after our HF etching. This unique surface characterization, by *in situ* SE, provides a useful means of studying and monitoring various Si surface conditions after HF cleaning.

The authors wish to thank Dr. Y. J. Chabal and AT&T Bell Laboratories for his helpful discussions. This work was partially supported by NASA-Lewis Grant NAG3-154.

[1] E. Yablanovitch, D. L. Allara, C. C. Chang, T. Gmitter, and T. B. Bright, Phys. Rev. Lett. 57, 249 (1986).
[2] M. Grundner and H. Jacob, Appl. Phys. A 39, 73 (1986).
[3] G. S. Higashi, Y. J. Chabal, G. W. Trucks, and K. Raghavachari, Appl. Phys. Lett. 56, 656 (1990).
[4] P. Jakob, P. Dumas, and Y. J. Chabal, Appl. Phys. Lett. 59, 2968 (1991).
[5] N. Hirashita, M. Kinoshita, I. Aikawa, and T. Ajioka, Appl. Phys. Lett. 56, 451 (1990).
[6] M. Morita, T. Ohmi, E. Hasegawa, M. Kawakami, and M. Ohwada, J. Appl. Phys. 68, 1272 (1990).
[7] P. Jakob and Y. J. Chabal, J. Chem. Phys. 95, 2897 (1991).
[8] R. M. A. Azzam and N. M. Bashara, *Ellipsometry and Polarized Light* (North-Holland, Amsterdam, 1977).
[9] D. E. Aspnes, in *Handbook of Optical Constants of Solids*, edited by E. D. Palik (Academic, New York, 1985), p. 89.
[10] G. H. Bu-Abbud, N. M. Bashara, and J. A. Woollam, Thin Solid Films 138, 27 (1986).
[11] H. Yaõ, P. G. Snyder, and J. A. Woollam, J. Appl. Phys. 70, 3261 (1991).
[12] D. E. Aspnes, J. Opt. Soc. Am. 64, 639 (1974).
[13] H. R. Philipp, Ref. 9, p. 759.
[14] G. E. Jellison, Jr., Opt. Mater. 1, 41 (1992).
[15] H. Yao and P. G. Snyder, Thin Solid Films 206, 283 (1991).
[16] H. Yao (unpublished data).
[17] D. E. Aspnes and J. B. Theeten, Phys. Rev. B 20, 3292 (1979).

HIGH FREQUENCY PERFORMANCE OF $Si_{1-x}Ge_x/Si_{1-y}Ge_y/Si_{1-x}Ge_x$ HBTs

D. Rosenfeld and S. A. Alterovitz

Indexing terms: Bipolar devices, Transistors, Semiconductor devices and materials

The results of a theoretical study of the performance of high speed SiGe HBTs is presented. The study includes a group of SiGe HBTs in which the Ge concentration in the base is 20% higher than that in the emitter and collector (i.e. $y = x + 0{\cdot}2$). It is shown that the composition dependences of f_T and the f_{max} are non-monotonic. As the Ge composition in the emitter and collector layers is increased, f_T and f_{max} first decrease, then remain constant and finally increase to attain their highest values.

Introduction: The main interest in SiGe alloys stems from their potential use in high speed heterostructure transistors for microwave and digital switching applications. In the last two decades a large number of HBTs based on III-V materials have been fabricated and characterised. However, it is only during the last few years that material growth and processing techniques compatible with silicon technology have been developed. The new SiGe growth technologies, as well as the recently published promising results of $Si/Si_{1-x}Ge_x/Si$ HBTs, have generated considerable need among material growers and device engineers for theoretical estimation of the potential performance of these SiGe devices. The composition dependence of the SiGe HBT figures of merit, such as the current gain, the cutoff frequency (f_T) and the maximum frequency of oscillation (f_{max}), has not been experimentally or theoretically estimated.

In this Letter, the results of a theoretical study of the composition dependence of f_T and f_{max} are presented. In the study, the high frequency characteristics of a series of *npn* SiGe HBTs with different emitter and collector compositions were calculated. To maintain the advantages of an HBT, the Ge concentration of the base in each of the HBTs was set to be 20% higher than that of the collector and emitter composition (i.e. $y = x + 0{\cdot}2$). The composition dependences of the emitter-to-collector transit time (τ_{ec}) and the base-resistance collector-capacitance product ($R_b C_c$) were computed and consequently, the dependences of f_T and f_{max} on the emitter and base compositions were derived.

Geometry and structure: We followed the design rules presented in Reference 1, and obtained device dimensions and dopant concentrations similar to those obtained in Reference 2. The chosen parameters were not meant to project the ultimate performance potential of SiGe HBTs and, therefore, the high frequency figures of merit are somewhat inferior to those recently published [3]. Because the study was comparative in nature all devices examined had the same areas (emitter and base $2 \times 8\,\mu m^2$, collector $10 \times 8\,\mu m^2$), same layer thicknesses (300, 500, 5000, 5000 Å in the emitter, base, collector and subcollector, respectively), same dopant profiles (10^{19}, 5×10^{18}, 10^{17} and $10^{20}\,cm^{-3}$) and same operating conditions (1 V base–collector bias). The HBTs differ in the emitter and collector Ge concentrations and in the base concentration, which was always set to be 20% higher than the former.

Device model and material properties: f_T and f_{max} were analysed using widely used formulas:

$$f_T = (2\pi \cdot \tau_{ec})^{-1} \quad (1)$$

$$f_{max} = (4\pi)^{-1} \cdot (\tau_{ec} \cdot R_b C_c)^{-1/2} \quad (2)$$

where τ_{ec} is given by

$$\tau_{ec} = \tau_e + \tau_b + \tau_{cib} + \tau_{sl} + \tau_c \quad (3)$$

In eqn. 3 τ_e and τ_c are the emitter and collector charging times, τ_b is the base transit time, τ_{cib} is the transit time associated with the current induced base at high current levels and τ_{sl} is the transit time through the base–collector depletion region (or collector–subcollector depletion region at high currents).

The above transit times depend strongly on the basic properties of the materials such as dielectric constants, mobilities, saturation velocities, bandgaps and dopant concentrations. The material properties, in turn, depend on the Ge concentration and hence it is expected that f_T and f_{max} will show a dependence on composition.

The SiGe material properties and their composition dependences were adopted from the literature. The resistances, the junction capacitances, and the built-in voltages were calculated using the expressions given in Reference 4. For the composition dependence of the bandgaps, the intrinsic carrier concentrations and the dielectric functions, we use the formulas published in References 5–7, respectively. The bandgap discontinuities and their composition dependences were taken from Reference 8. The expressions for the carrier mobilities in SiGe are based on the theoretical calculation presented in Reference 9. For the saturation velocity of electrons in SiGe alloys we employed a linear fit between the saturation velocities of electrons in Si and Ge. The influence of the high current on the width and location of the base–collector depletion region was calculated according to Reference 10.

Results and discussion: The calculated f_T and f_{max}, plotted against the collector current density J_c for several SiGe HBTs, are shown in Figs. 1 and 2. All transistors were identical in

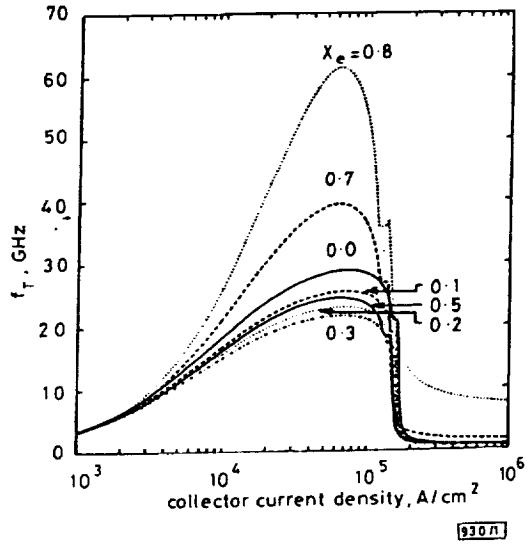

Fig. 1 *Cutoff frequency f_T of $Si_{1-x}Ge_x/Si_{1-y}Ge_y/Si_{1-x}Ge_x$ HBTs against collector current density, plotted for several values of emitter composition*

$X_c = X_e$ and $X_b = X_e + 0{\cdot}2$

geometry and dopant profile. However, they differed in the compositions of the layers. The emitter and collector compositions were varied from $X_e = X_c = 0$ to $X_e = X_c = 0{\cdot}8$ and the base composition varied from 0·2 to 1.

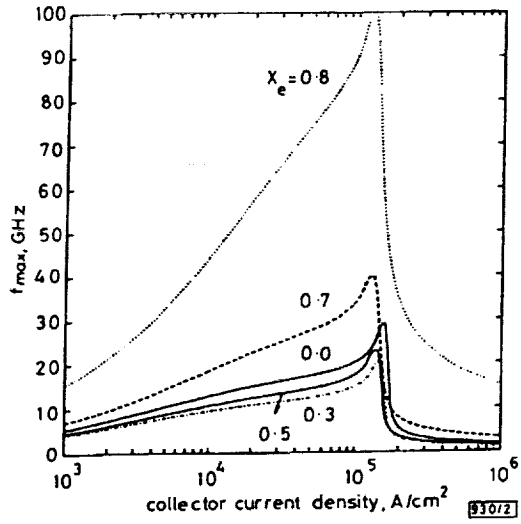

Fig. 2 *Maximum oscillation frequency f_{max} of $Si_{1-x}Ge_x/Si_{1-y}Ge_y/Si_{1-x}Ge_x$ HBTs against collector current density, plotted for values of emitter composition*

$X_c = X_e$ and $X_b = X_e + 0{\cdot}2$

Figs. 1 and 2 demonstrate the non-monotonic behaviour of both f_T and f_{max}. For $X_e = 0$ (pure silicon in the emitter and collector), the highest f_T and f_{max} (29 GHz) are obtained at collector currents of 72 kA cm^{-2} and 162 kA cm^{-2}, respectively. Increasing the emitter and collector compositions to 0·4 (and the base composition to 0·6), the highest f_T and f_{max} *decrease* to 23 GHz, and are obtained for collector currents of 68 kA cm^{-2} and 150 kA cm^{-2}. Further increasing the emitter composition to 0·8 (and pure Ge in the base), the peak values

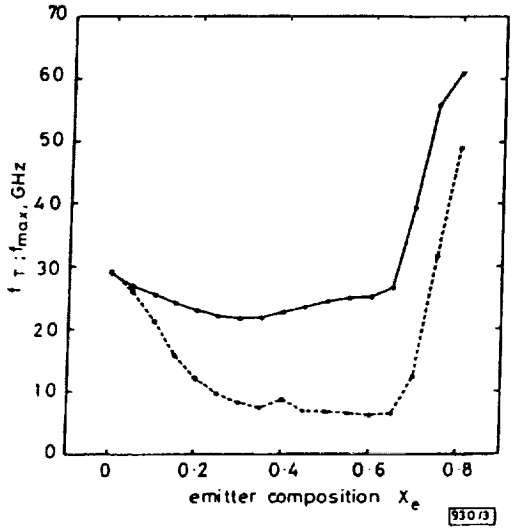

Fig. 3 *f_T at $J_c = 72$ A cm^{-2} and f_{max} at $J_c = 162$ A cm^{-2} against emitter composition*

At these current densities f_T and f_{max} attain their highest values for $X_e = 0{\cdot}2$

——— f_T at 72 kA/cm^2

- - - - f_{max} at 162 kA/cm^2

of f_T and f_{max} *increase* to 62 and 100 GHz, obtained for $J_c =$ 72 kA cm^{-2} and 162 kA cm^{-2}. Fig. 3 emphasises the non-monotonic behaviour of f_T and f_{max}, by showing the f_T and f_{max} values (calculated for $J_c = 72$ kA cm^{-2} and $J_c =$ 172 kA cm^{-2}, respectively), plotted against the emitter composition.

Conclusion: We have demonstrated the non-monotonic behaviour of f_T and f_{max}. As the Ge composition in the emitter and collector layers (as well as the base) is increased, f_T and f_{max} first decrease, then remain almost constant and finally increase to attain their highest values.

6th November 1992

D. Rosenfeld* and S. A. Alterovitz (*NASA—Lewis Research Center, Mail Stop 54-5, 21000 Brookpark Rd., Cleveland, OH 44135, USA*)

* National Research Council Resident at NASA—Lewis Research Center, USA. Permanent address: Faculty of EE, Technion IIT, Haifa 32000, Israel

References

1 PATTON, G. L., COMFORT, J. H., STORK, B. S., MEYERSON, B. S., CRABBE, E. F., SCILLA, G. J., DEFRESART, E., STORK, J. M. C., SUN, J. Y. C., HARMAN, D. L., and BURGHARTZ, J. N.: '75 GHz f_t SiGe-base heterojunction bipolar transistors', *IEEE Electron Device Lett.*, 1990, EDL-11, pp. 171–173

2 CHEN, J., GAO, G. B., and MORKOC, H.: 'Comparative analysis of the high frequency performance of $Si/Si_{1-x}Ge_x$ heterojunction and Si bipolar transistors', *Solid-State Electron.*, 1992, 35, pp. 1037–1044

3 CRABBE, E. F., COMFORT, J. H., LEE, W., CRESSLER, D., MEYERSON, B. S., MEGDANIS, A. C., SUN, J. Y. C., and STORK, M. C.: '73 GHz self aligned SiGe base bipolar transistors with phosphorus doped polysilicon emitters', *IEEE Electron Device Lett.*, 1992, 13, pp. 259–261

4 MILNES, A. G., and FEUCHT, D. L.: 'Heterojunctions and metal-semiconductors junctions' (Academic Press, New York, 1972), pp. 34–94

5 KARLSTEEN, M., and WILLANDER, M.: 'Optimized frequency charcterisetics of Si/SiGe heterojunction and conventional bipolar transistors', *Solid-State Electron.*, 1990, 33, pp. 199–204

6 KLAUSMEIER-BROWN, M. E., LUNDSTROM, M. N., and MELLOCH, M. R.: 'The effects of heavy impurity doping on AlGaAs/GaAs bipolar transistors', *IEEE Trans.*, 1989, ED-36, pp. 2146–2155

7 SUTHERLAND, J. E., and HAUSER, J. R.: 'A computer analysis of heterojunction and graded composition solar cells', *IEEE Trans.*, 1977, ED-24, pp. 363–372

8 PEOPLE, R., and BEAN, J. C.: 'Band alignment of coherently strained Ge_xSi_{1-x}/Si heterostructures on ⟨001⟩ Ge_ySi_{1-y}', *Appl. Phys. Lett.*, 1986, 48, pp. 538–540

9 KRISHMANURTHY, S., CHER, A., and CHEN, A.: 'Generalized Brooks' formula and the electron mobility in Ge_xSi_{1-x} alloys', *Appl. Phys. Lett.*, 1985, 47, pp. 160–162

10 ROULSTON, D. J.: 'Bipolar semiconductor devices' (McGraw-Hill Publishing Company, NY, NY, 1990), pp. 254–258